1993PASP..105..501H

Publications of the Astronomical Society of the Pacific
105: 501–508, 1993 May

Large Astronomical Liquid Mirrors

PAUL HICKSON, BRAD K. GIBSON, AND DAVID W. HOGG

Department of Geophysics and Astronomy, 2219 Main Mall, University of British Columbia,
Vancouver, British Columbia, V6T 1Z4, Canada
Electronic mail: paul@geop.ubc.ca, gibson@geop.ubc.ca, hogg@geop.ubc.ca

Received 1992 November 6; accepted 1993 February 25

ABSTRACT. We present a design for large rotating liquid mirrors. These mirrors are stiff lightweight structures designed to support a thin reflective mercury surface layer. The general design features and fabrication techniques are described and approximate analytic formulas are derived describing the flexural, vibrational, and stability characteristics of these mirrors. As an example, we describe in detail the 2.7-m mirror of the UBC/Laval liquid mirror observatory. We conclude by considering the feasibility of employing this design for very large liquid mirrors.

1. INTRODUCTION

The recent demonstration of a diffraction-limited 1.5-m rotating liquid mercury mirror (Borra et al. 1989), opened a new era in the design of large ground-based zenith-pointing optical telescopes. This development combined with the advent of large-format CCD detectors which can compensate for the Earth's rotation by operating in a time-delay integration or drift-scanning mode (McGraw et al. 1980; Wright and McKay 1981; Gibson and Hickson 1992), makes the serious consideration of large liquid mirror telescopes (LMTs) possible.

Liquid mercury can provide an excellent surface for the reflection of light. The reflectivity of mercury ranges from 79% at 3100 Å to 90% at 13,000 Å (Hass and Hadley 1963; Schultz 1957) making it competitive with aluminum, particularly in the red region of the spectrum. Mercury has some inherent advantages over aluminum in that its surface can be cleaned regularly to maintain a high reflectivity whereas large aluminum mirrors are rarely realuminized more than once per year and suffer some degredation due to oxidation and the presence of dust. Although mercury vapor is toxic, Borra et al. (1992) find that, within several hours, a transparent surface layer forms on the mercury which supresses evaporation to below detectable limits. It is therefore unlikely that mercury toxicity will present a serious problem.

Large LMTs may offer an economical alternative to conventional telescopes for certain projects such as wide-area surveys. Because of the relatively low cost and simplicity of the liquid mirrors, it may in the near future be possible to build LMTs with greater collecting area than even the largest conventional telescopes.

Work involving liquid mirrors is being conducted by several groups (Borra et al. 1992; Vasil'ev 1985; Potter 1991). The largest astronomical liquid mirror of which we are aware is that of the 2.7-m LMT collaboration of the University of British Columbia (UBC) and Laval University (Gibson and Hickson 1991; Hickson et al. 1990). Located near Vancouver, this telescope saw first light in 1992 September and is expected to become operational by 1993. Its primary scientific role will be in conducting surveys of galaxies and quasars in a 20′ wide band of sky centered at approximately 49° declination. The telescope, and associated scientific programs will be described in detail in future papers. In this paper we describe the design and construction of the mirror.

Borra (1982) has shown that in order to obtain good image quality, the angular velocity of rotation must be uniform to within $\sim 10^{-5}$, and the surface of the mercury must be free of vibration-induced surface waves and other nonuniformities, to within a fraction of wavelength of light. This may be achieved by supporting the mirror with an air bearing and driving it by a synchronous motor controlled by a quartz oscillator. Borra et al. (1992) have also developed a technique which allows a relatively thin (~ 2 mm) mercury layer to be used, thereby reducing the weight of the mirror significantly.

In larger liquid mirrors of this type, three design constraints become particularly severe. First, the mirror must support a heavier mercury load without undue flexing. In particular, the mirror flexure should be less than of order 1/10 of the thickness of the mercury layer. At the same time, the entire structure must be as light as possible, to allow it to be supported by an air, or possibly an oil, bearing. Second, both the mirror, and its support system must be stiff in torsion about a horizontal axis in order to avoid instability that can result from the horizontal flow of mercury due to tilt of the mirror axis (Content 1992). Finally, the fundamental resonant frequency of the mirror must be as high as possible, in order to suppress the amplitude of surface waves caused by any small vibrations transmitted to the mirror. Thus, it is very important that the mirror be relatively light yet stiff, and have high intrinsic vibration damping.

In this paper we describe a mirror design which has sucessfully met these criteria for diameters as large as 3 m. Developed originally for the UBC/Laval 2.7-m LMT, it has been the basis for the construction of four large liquid mirrors. Two 2.7-m mirrors, one for the UBC/Laval LMT and one for the University of Western Ontario Lidar Facility, and a 3.0-m mirror for NASA (Hickson 1993) were built at UBC, and a 2.5-m liquid mirror has been built at Laval University (Borra 1992a).

The basic design is described in Sec. 2, and its mechan-

© 1993. Astronomical Society of the Pacific

© Astronomical Society of the Pacific • Provided by the NASA Astrophysics Data System

1993PASP..105..501H

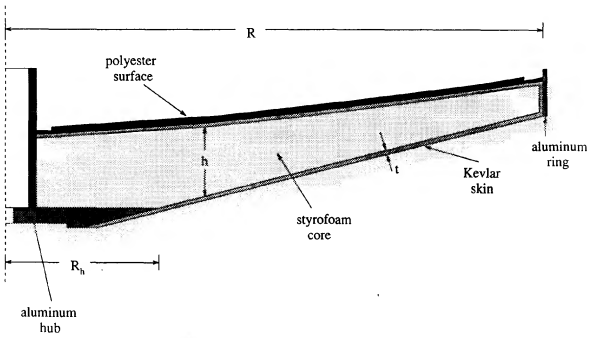

FIG. 1—Mirror cross section showing structural elements. The upper surface is parabolic and supports a thin mercury layer. Depressions seen in the upper surface are grooves needed to overcome surface tension effects at the inner and outer edges of the mercury layer.

ical characteristics are evaluated. Section 3 describes the construction techniques used in building the 2.7-m mirror, and in Sec. 4 we consider larger mirrors and discuss modifications to the basic design which might allow the construction of mirrors with diameters as large as 8 m.

2. MIRROR DESIGN

2.1 Mechanical Design

The essential structural elements of our design are shown in Fig. 1. The mirror is of composite construction, consisting of a strong skin surrounding a lightweight core. An aluminum hub serves to stiffen the central region of the mirror, and allows precise centering of the mirror on the air bearing and drive system. An aluminum ring attached to the rim of the mirror retains the mercury. The rim also contains hard points for the attachment of balance weights. The upper surface of the mirror is filled to a depth of ~ 1 cm with a spun-cast layer of polyester resin which supports the mercury.

The skin of the mirror, which bears tensile and compressive stresses, consists of structural fibers in an epoxy matrix. Several types of materials are available for use as reinforcing fibers, the most appropriate being woven fabrics consisting of fibers of glass, Kevlar, or graphite. Fiberglass is the least expensive and is simple to work with, but gives lower performance than the other fabrics. For example, Kevlar has a modulus of elasticity about 50% greater than that of Fiberglass and weighs 15% less. However, its cost is about three times that of Fiberglass. Graphite has an elastic modulus about 30% greater than that of Kevlar, and a comparable density. Its cost is currently about three times that of Kevlar. For small mirrors Kevlar is probably the most suitable choice. For large mirrors, graphite may be more suitable because of its higher specific stiffness. All these materials are available in a range of fabric types with bidirectional (BID) or unidirectional weaves. The former has comparable stiffness and strength in directions parallel and perpendicular to the weave and is most suitable for covering surfaces with compound curvature.

Because these fabrics are anisotropic, several layers must be used with different orientation angles to give a skin which has roughly homogeneous mechanical properties. The upper and lower skins of the 2.7-m mirror consist of four plys of Kevlar-49, type 281, BID cloth oriented 22.5° to each other. These plys overlap 10 cm at the rim of the mirror, and overlap 5 cm onto the aluminum hub. Two additional plys extend from the center of the mirror to 2/3 of its radius and 2 more plys extend from the center to 1/3 of the radius.

TABLE 1
Material Properties

material	ρ (kg/m^3)	E (GPa)	σ (GPa)
Fiberglass[1]	1513	16.0	0.35
Kevlar[2]	1179	22.3	0.36
graphite[3]	1280	29.0	0.36
styrofoam	32	0.02	0.35
epoxy[4]	1140	3.32	0.45

Notes:
1. Type RA7725 BID E-glass fabric in epoxy matrix
2. Kevlar 49 type 281 BID fabric in epoxy matrix
3. Type 584 BID graphite fabric in epoxy matrix
4. Hexcel 2410/2183 epoxy/hardener 100/45 volume ratio

Shear stresses are borne by the core of the mirror which consists of a lightweight material. A variety of core materials are available. For small mirrors Dow styrofoam is probably the most convenient. It is lightweight, rigid, and has the additional advantage of being relatively easy to shape and assemble. For much larger mirrors, a material with a higher shear modulus than styrofoam must be used.

Mechanical properties of various structural materials are listed in Table 1. The columns give density (ρ), Young's modulus (E), and Poisson's ratio (σ). For the composite materials, these figures refer to azimuthally averaged properties appropriate to the approximately homogeneous multi-ply skins described above. As these properties depend to some degree on the construction techniques used, they were determined by laboratory measurement of test samples (Hickson et al. 1993).

As can be seen in Fig. 1, the bottom of the mirror has a conical shape. This provides increased rigidity while keeping the weight to a minimum. It also results in the thickness of the mirror being approximately constant, because of the parabolic shape of the upper surface, which simplifies the structural analysis.

2.2 Structural Analysis

The cylindrical symmetry of the mirror allows key structural properties to be estimated analytically (Appendix). This approximation is reasonable providing that shear deformation in the core can be neglected. For axisymmetric deformations, the condition that must be satisfied is

$$htE_s(1-\sigma_c)/R^2E_c \ll 1, \qquad (1)$$

where R is the mirror radius, t and E_s are the thickness and Young modulus of the skin, and h, E_c, and σ_c are the thickness, Young modulus, and Poisson ratio of the core. For dipole deformations, corresponding to an axis tilt, stiff-

© Astronomical Society of the Pacific • Provided by the NASA Astrophysics Data System

1993PASP..105..501H

ness of the central portion is most important, and the thin-plate condition is

$$\frac{htE_s(1-\sigma_s)}{R_h^2E_c} \ll 1, \tag{2}$$

where R_h is the radius of the metal hub. When the above conditions are satisfied, we obtain the following results:

The ratio of the maximum deflection of the mirror to the thickness of the mercury layer (the *deflection coefficient*) is given by the formula

$$\frac{\zeta_{\max}}{t_{\rm Hg}} = \frac{7+3\sigma_s}{64D(1+\sigma_s)} \rho_{\rm Hg} g R^4 \eta(\mu), \tag{3}$$

where $\rho_{\rm Hg}$ is the density of mercury (13,596 kg m^{-3} at 0° C), g is the gravitational acceleration, and D is the coefficient of rigidity, given by

$$D = \frac{E_s h^2 t}{2(1-\sigma_s^2)}, \tag{4}$$

where $\eta(\mu)$ is a function which contains the dependence of the deflection on the ratio $\mu = R_h/R$ of the hub radius to mirror radius (Fig. 1). For the 2.7 m mirror, $\mu = 0.15$ and $\eta = 0.67$.

The fundamental resonant frequency of the mirror may be estimated from the formula

$$f_0^\nu = \frac{1}{2\pi}\sqrt{\frac{\lambda_0^\nu D}{m}}, \tag{5}$$

where m is the mass per unit surface area of the mirror and mercury, and λ_0^ν depends on μ and the azimuthal mode number ν. Dimensionless resonant frequencies $\hat{f}_0^\nu = f_0^\nu (mR^4/D)^{1/2}$ for several modes are plotted in Fig. 4. For the 2.7 m mirror the lowest frequency mode is the dipole $\nu = 1$, and $\hat{f}_0^1 = 0.656$.

In order to avoid instability due to the horizontal flow of mercury, both the mirror and the support system must be sufficiently stiff. The condition for stability is

$$\gamma^1 + \gamma_s \leqslant 1, \tag{6}$$

where γ^1 is the dipole flexure coefficient for the mirror

$$\gamma^1 = \frac{g\rho_{\rm Hg}R^4}{(2\pi\hat{f}_0^1)^2 D} \tag{7}$$

and γ_s is the flexure coefficient for the support system

$$\gamma_s = \frac{4\kappa}{\pi g \rho_{\rm Hg} R^4}. \tag{8}$$

Here κ is the moment stiffness of the support system, i.e., the restoring torque per radian of axis tilt. Flexure coefficients for the mirror design presented here may be determined, for any value of μ, from the $\nu = 1$ curve of Fig. 4. For the 2.7 m mirror $\gamma^1 = 0.06 g\rho_{\rm Hg}R^4/D = 0.07$.

The mechanical characteristics of the UBC/Laval 2.7-m mirror are shown in Table 2. The predicted value of the deflection coefficient, from (3) is 0.11. Laboratory measurement of the completed mirror indicated a deflection coefficient of 0.13. The small difference is likely a result of shear deformation since for this mirror $htE_s(1-\sigma_c)/R^2E_c \simeq 0.2$. For the 2.7-m mirror, the thin-plate approximation fails badly for dipole deflections as $htE_s(1-\sigma_c)/R_h^2E_c \simeq 9$. As a result, the predicted dipole flexure coefficient ($\gamma^1 = 0.07$) is considerably lower than the measured value of 0.22.

TABLE 2
Mechanical Characteristics of the UBC/Laval 2.7-m Mirror

parameter	value
radius (R)	1.33 m
hub radius (R_h)	0.20 m
core thickness (h, typical)	0.12 m
skin thickness (t, central)	2.0 mm
focal length	5.00 m
mass (empty)	120 kg
mass (with 2mm Hg)	270 kg
deflection factor (ζ_{max}/t_{Hg})	0.13
dipole flexure coefficient (γ^1)	0.22
resonant frequency (empty)	27 Hz
resonant frequency (with 2mm Hg)	18 Hz

The lowest resonant frequency occurs for dipole vibrations. For the 2.7-m mirror, the thin-plate approximation predicts a resonant frequency of 48 Hz with no mercury load and 32 Hz with a 2 mm thick mercury layer. Because of shear deformation, the true values are expected to be lower by a factor of $1.8(\sqrt{0.22/0.07})$.

The principal factors determining the strength are the thickness of the core and skins, the strength of the skin, and the diameter of the hub. As can be seen from the above formulas, for a given mirror diameter, the stiffness increases in proportion to the skin thickness and the square of the core thickness. The deflection and flexure coefficients are inversely proportional to the stiffness, but the resonant frequency increases only as the square root of the stiffness. The design can be scaled homologously to larger mirrors. The deflection, flexure coefficients, and (approximately) the resonant frequency, are unchanged when the skin thickness increases in proportion to the square of the mirror radius, $t \propto R^2$, as long as the thin-plate conditions (1) and (2) are met. It may, of course, be more practical to modify the design for large mirrors, by increasing the relative thickness h/R, for example. In addition, increasing the diameter of the aluminum hub improves the mirror performance significantly. The hub should therefore be made as large as is practical.

3. CONSTRUCTION TECHNIQUES

Fabrication of the mirror follows standard techniques of composite construction (e.g., Marshall 1989). For the 2.7-m mirror, construction proceeded as follows: Core segments were cut from blocks of styrofoam using a hot-wire cutter. This consisted of a 1.2-m length of 1 mm diameter stainless-steel wire stretched on a light rigid frame and connected to the secondary circuit of a variable transformer. After cutting, the individual segments were aligned and glued together by two-component polyurethane foam. After assembly and bonding to the aluminum hub, the circumference of the foam core was trimmed by fixing the hotwire in a vertical position, then rotating the entire foam

© Astronomical Society of the Pacific • Provided by the NASA Astrophysics Data System

1993PASP..105..501H

core on the mirror bearing. In a similar manner, the bottom surface of the foam core was trimmed to the conical shape.

Lamination of the Kevlar skin began with the lower surface. The mirror was inverted and the foam surface was prepared by filling any small dents or cracks in the core with polyurethane foam and sanding the entire lower surface and rim of the core as well as the metal hub that would be bonded to the skin. Pores in the foam were then filled with a light mixture of epoxy and glass microspheres. Consecutive layers of Kevlar cloth were then applied and laminated with Hexcel type 2410 resin and type 2183 hardener. This resin has relatively low toxicity, low exothermic heat production, and minimal shrinkage upon curing.

When the lower Kevlar skin had cured (about 24 hr at 25 °C), the mirror was placed right side up on the bearing. The upper surface of the foam core was then machined to produce an accurate parabola. For the UBC 2.7-m and NASA 3.0-m mirrors, this was done by employing a two-axis translation stage carrying a rotating cutter.

After machining, the upper surface of the mirror was prepared and covered with Kevlar in the same manner as the lower surface. The upper and lower skins overlap 10 cm on the rim. When the epoxy had cured, blind nuts were installed, to provide attachment points for the metal rim and counterweights. The nuts for the 2.7-m mirror were made from 2.5 cm diameter stainless-steel disks containing tapped holes to receive screws which hold the metal rim of the mirror, in addition to larger holes for balance weight bolts. They were installed by first cutting oversized holes through the Kevlar skin and into the foam around the mirror circumference. The metal rim and blind nuts were glued to the rim of the mirror with flox—a mixture of cotton fibers and epoxy. A final strip of Kevlar was applied to the upper surface, lapping up over the metal rim in order to securely bond the rim.

The final surface of the mirror was formed by spincasting. Borra (1992b) has found that Hexcel type 3138 polyurethane resin is suitable for spincasting large mirrors. The resin and hardener were mixed by hand, to avoid air entrainment which would result in bubbles, and applied in one operation while the mirror was rotating.

The completed 2.7-m mirror is shown in Fig. 2. The mirror is covered with a 2 mm thick mercury layer with a surface of high optical quality. The mirror is being supported by a Rank–Pneumo model RT-14002 14″ air bearing. The mirror has recently been tested and found to be of excellent quality, producing star images with half-widths of less than 2 arcsec, limited only by the atmospheric seeing.

FIG. 2—The completed 2.7-m mirror, rotating on its air bearing, supporting a 2 mm thick mercury layer of optical quality.

4. DISCUSSION

Although approximations were made in deriving the formulas presented here, the results should be of sufficient accuracy to allow an evaluation of the design. A finite element analysis has been made of a mirror design similar to this one by Arrien (1990). His results are in general agreement with the analytic formulas and confirm the excellent structural performance of this type of mirror.

When considering the scaling of this design to larger mirrors, several factors must be considered. For homologous scaling, where h/R and R_h/R are fixed, the skin thickness t must increase as R^2. However, it is essential that the stability condition (6) be met. Since the stiffness of the mirror against dipole distortions depends strongly on the rigidity of the hub and central region of the mirror, it is important that shear deformation be minimized. In particular, the conditions (1) and (2) must be satisfied, despite the increase in t. It will therefore be necessary to adopt a core structure which has a significantly higher shear modulus than styrofoam, at least in the central region of the mirror. Possible solutions include a composite or metal honeycomb core, or a network of composite fiber-reinforced ribs. Considerable gains can be made by making the metal hub as large as possible. By increasing $\mu = R_h/R$, the relative flexure (η) is reduced, and the thin-plate condition (2) becomes less stringent. Further gains may be obtained by making the hub symmetric, with an upper diameter as large as the lower diameter. Cost savings can also be realized by adopting a skin thickness that decreases with radius. Further discussion of these and related topics is given by Hickson (1993).

Some weight and cost savings would occur if the spuncast surface layer could be eliminated. This could possibly be done by constructing the mirror upside down on top of a carefully made and rigidly supported parabolic mold which would give the desired surface finish. Such a mold could be machined, or made from a spuncast mirror. This may be a particularly attractive way to make mirrors for an array where the cost of making the mold is offset by the savings in manufacturing the individual mirrors. Another option for very large mirrors, would be to make individual segments, each covered with a Kevlar or graphite skin. All segments could be made from a single mold and then joined to form a complete mirror. This could also be a cost-effective way to produce arrays of large liquid mirrors.

The design described here has been used to make successful mirrors of up to 3 m in diameter. By increasing size and stiffness of the hub, it should be possible to employ this

© Astronomical Society of the Pacific • Provided by the NASA Astrophysics Data System

1993PASP..105..501H

basic design for mirrors in the 4 to 5 m class. By adopting stiffer core materials, and graphite skins, it may be possible to extend this design to mirrors of the 8 to 10 m class.

We thank L. Robertson and R. Content for comments on an earlier version of the manuscript. This work was supported by grants from the Natural Sciences and Engineering Research Council of Canada.

APPENDIX: MIRROR STRUCTURAL ANALYSIS

An analytic structural analysis of the mirror can be made by assuming that the mirror thickness h and skin thickness t are constant. In our design h typically varies with radius by less than 20%. The assumption of constant t, is also not a bad one. Numerical calculations (Hickson 1993) indicate that flexure with a skin whose thickness decreases linearly with radius to half the central value is less than 15% greater than flexure with a constant-thickness skin. So while it is more efficient to allow the thickness t to decrease with radius, the results can be approximated by constant t when t is taken to be the central thickness.

Because of the homogeneity of its construction, the free portion of the mirror (that not supported by the hub) may be treated as a thin (almost) flat plate undergoing deflection due to a uniform pressure P normal to its surface. In this approximation, shear deformations within the core are assumed to be negligible. We therefore require that the ratio of shear deformation to skin extension be small. For axisymmetric flexure, this gives the condition

$$htE_s(1-\sigma_c)/R^2E_c \ll 1, \tag{9}$$

where R is the mirror radius, E is Young's modulus, σ is Poisson's ratio, and the subscripts c and s refer to the core and skin, respectively. For dipole deformations (corresponding to an axis tilt), stresses are concentrated near the hub, so the more stringent condition

$$htE_s(1-\sigma_c)/R_h^2E_c \ll 1, \tag{10}$$

where R_h is the radius of the hub, applies.

Under the flat-plate approximation (in cylindrical coordinates r,ϕ,z), with the z axis coinciding with the symmetry axis of the mirror, the perpendicular deflection $\zeta(r)$ satisfies the equation

$$D\Delta^2\zeta = P, \tag{11}$$

where Δ^2 is the biharmonic operator

$$\Delta^2 = \left(\frac{1}{r}\frac{\partial}{\partial r}r\frac{\partial}{\partial r}+\frac{1}{r^2}\frac{\partial^2}{d\phi^2}\right)^2, \tag{12}$$

and D is the flexural rigidity

$$D = \int_{-h/2}^{h/2}\frac{E}{1-\sigma^2}z^2\,dz \tag{13}$$

(see, for example, Landau and Lifshitz 1959). Performing the integration, D becomes

$$D = \frac{E_s h^2 t}{2(1-\sigma_s^2)}+\frac{E_c h^3}{12(1-\sigma_c^2)}. \tag{14}$$

Because Kevlar has a much higher Young's modulus than styrofoam, the second term contributes typically less than 1% of the total stiffness.

We assume that the central area of the mirror, within the radius R_h of the hub is rigidly supported, and that the rim of the mirror is free. At the inner edge, $r=R_h$ we have the inner boundary conditions

$$\zeta = 0, \tag{15}$$

$$\frac{\partial\zeta}{\partial r} = 0, \tag{16}$$

and at the rim of the mirror, $r=R$, we have the outer boundary conditions

$$\frac{\partial}{\partial r}\Delta\zeta+\frac{(1-\sigma)}{r}\frac{\partial}{\partial r}\frac{1}{r}\frac{\partial^2\zeta}{\partial\phi^2} = 0, \tag{17}$$

$$\frac{\partial^2\zeta}{\partial r^2}+\frac{\sigma}{r}\frac{\partial\zeta}{\partial r}+\frac{\sigma}{r^2}\frac{\partial^2\zeta}{\partial\phi^2} = 0, \tag{18}$$

where Δ is the Laplacian operator

$$\Delta = \frac{1}{r}\frac{\partial}{\partial r}r\frac{\partial}{\partial r}+\frac{1}{r^2}\frac{\partial^2}{\partial\phi^2}. \tag{19}$$

The general solution may be written

$$\zeta = \xi+\beta, \tag{20}$$

where ξ is a particular solution of the inhomogeneous equation (11) and β is the general solution of the biharmonic equation $\Delta^2\beta=0$, and has the form

$$\beta = \sum_{\nu=0}^{\infty}\chi^\nu(r)e^{i\nu\phi}, \tag{21}$$

where ν is a positive integer and

$$\begin{aligned}
\chi^0 &= a_0^0 r^2+a_1^1 r^2\ln r+a_2^0\ln r+a_3^0, \quad \nu=0,\\
\chi^1 &= a_0^1 r^3+a_1^1 r+a_2^1 r\ln r+a_3^1/r, \quad \nu=1,\\
\chi^\nu &= a_0^\nu r^{2+\nu}+a_1^\nu r^\nu+a_2^\nu r^{2-\nu}+a_3^\nu r^{-\nu}, \quad \nu>1,
\end{aligned} \tag{22}$$

where the a_i^ν $(i=0,1,2,3)$ are constants determined by the boundary conditions (10)–(13). For loads of the form

$$P = Ar^n e^{i\nu\phi}, \tag{23}$$

a particular solution is

$$\xi = \frac{A}{[(n+4)^2-\nu^2][(n+2)^2-\nu^2]}r^{n+4}. \tag{24}$$

1. Deflection

For the simple case of a uniform mercury load $P=g\rho_{\rm Hg}t_{\rm Hg}$, where $\rho_{\rm Hg}$ and $t_{\rm Hg}$ are the density and depth of the mercury layer and g is the gravitational acceleration, the deflection is

© Astronomical Society of the Pacific • Provided by the NASA Astrophysics Data System

1993PASP..105..501H

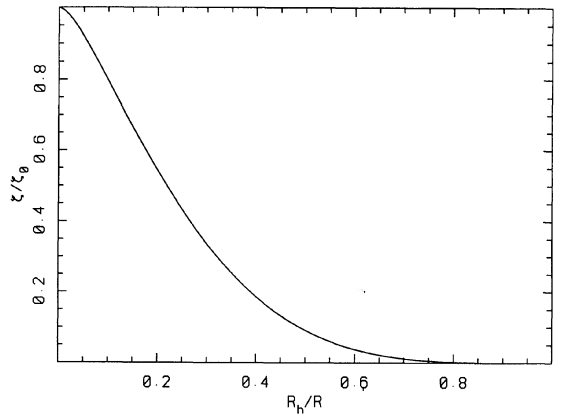

FIG. 3—Relative deflection of the mirror, under a uniform mercury load, as a function of the relative hub diameter $\mu=R/R_h$.

$$\zeta=\frac{PR^4}{64D}\left\{x^4-\mu^4-8(x^2\ln x-\mu^2\ln\mu)+\frac{2}{1+\sigma+(1-\sigma)\mu^2}[(3+\sigma)\{x^2-\mu^2-2\mu^2\ln(x/\mu)\}-\mu^2(\mu^2-4\ln\mu-2)\{(1-\sigma)(x^2-\mu^2)+2(1+\sigma)\ln(x/\mu)\}]\right\},\quad \mu\leqslant x\leqslant 1,$$

$$\zeta=0,\quad 0\leqslant x\leqslant\mu, \tag{25}$$

where $x=r/R$ and $\mu=R_h/R$.

The maximum deflection occurs at the rim ($x=1$), and has the form

$$\zeta_{\max}=\zeta_0\eta(\mu), \tag{26}$$

where

$$\zeta_0=\frac{7+3\sigma}{64D(1+\sigma)}PR^4, \tag{27}$$

and $\eta(\mu)=\zeta(x=1,\mu)/\zeta(x=1,\mu=0)$ is plotted in Fig. 3. It is evident from the figure that the deflection decreases rapidly as the relative diameter of the hub increases, being about a factor of two smaller for $\mu=0.2$.

Since the deflection is proportional to the pressure P which is in turn proportional to the thickness $t_{\rm Hg}$ of the mercury layer, it is convenient to define a dimensionless *deflection factor* as the ratio of the maximum deflection to the thickness of the mercury layer

$$\frac{\zeta_{\max}}{t_{\rm Hg}}=\frac{7+3\sigma}{64D(1+\sigma)}\rho_{\rm Hg}gR^4\eta(\mu). \tag{28}$$

It should be noted that the deviation of the surface from parabolicity is considerably less than the deflection, being less than $0.1\zeta_{\max}$ over almost the entire range of μ.

2. Vibration

Vibrations of the mirror about its equilibrium position may be treated by making the replacement

$$P=-m\frac{\partial^2\zeta(t)}{\partial\tau^2} \tag{29}$$

in Eq. (11). Here τ is time and m is the mass per unit surface area of the mirror, assumed to be constant.

Writing

$$\zeta(\tau)=\zeta\cos(\omega\tau) \tag{30}$$

(with ζ implicitly a function of r and ϕ), we obtain

$$\Delta^2\zeta=\lambda\zeta, \tag{31}$$

where

$$\lambda=\frac{m}{D}\omega^2. \tag{32}$$

Thus, the vibrational modes of the mirror are the eigenfunctions of the biharmonic operator, with characteristic frequencies given by

$$\omega=\sqrt{\frac{\lambda D}{m}}. \tag{33}$$

The most general eigenfunction is

$$\zeta=[a_0I_\nu(kr)+a_1J_\nu(kr)+a_2K_\nu(kr)+a_3Y_\nu(kr)]e^{i\nu\phi}, \tag{34}$$

where I_ν, J_ν, K_ν, and Y_ν are the usual Bessel and modified Bessel functions and $k^4=\lambda$. a_0, a_1, a_2, and a_3 are constants to be determined from the boundary conditions. The condition that ζ be single-valued requires that ν take only integer values.

Substituting (34) in Eqs. (15)–(18), and using well-known properties of the Bessel functions gives the equations

$$I_\nu(\mu x)a_0+J_\nu(\mu x)a_1+K_\nu(\mu x)a_2+Y_\nu(\mu x)a_3=0,$$

$$\{\nu I_\nu(\mu x)+\mu xI_{\nu+1}(\mu x)\}a_0+\{\nu J_\nu(\mu x)-\mu xJ_{\nu+1}(\mu x)\}a_1+\{\nu K_\nu(\mu x)-\mu xK_{\nu+1}(\mu x)\}a_2+\{\nu Y_\nu(\mu x)-\mu xY_{\nu+1}(\mu x)\}a_3=0,$$

$$\{[\nu^2(1-\nu)(1-\sigma)+\nu x^2]I_\nu(x)-[\nu^2(1-\sigma)-x^2]xI_{\nu+1}(x)\}a_0+\{[\nu^2(1-\nu)(1-\sigma)-\nu x^2]J_\nu(x)+[\nu^2(1-\sigma)+x^2]xJ_{\nu+1}(x)\}a_1+\{[\nu^2(1-\nu)(1-\sigma)+\nu x^2]K_\nu(x)+[\nu^2(1-\sigma)-x^2]xK_{\nu+1}(x)\}a_2+\{[\nu^2(1-\nu)(1-\sigma)-\nu x^2]Y_\nu(x)+[\nu^2(1-\sigma)+x^2]xY_{\nu+1}(x)\}a_3=0,$$

© Astronomical Society of the Pacific • Provided by the NASA Astrophysics Data System

1993PASP..105..501H

$$\{[\nu(1-\nu)(1-\sigma)-x^2]I_\nu(x)+(1-\sigma)xI_{\nu+1}(x)\}a_0+\{[\nu(1-\nu)(1-\sigma)+x^2]J_\nu(x)-(1-\sigma)xJ_{\nu+1}(x)\}a_1$$
$$+\{[\nu(1-\nu)(1-\sigma)-x^2]K_\nu(x)-(1-\sigma)xK_{\nu+1}(x)\}a_2+\{[\nu(1-\nu)(1-\sigma)+x^2]Y_\nu(x)-(1-\sigma)xY_{\nu+1}(x)\}a_3=0, \quad (35)$$

where $x=kR$ and μ is the ratio of inner to outer radii. These are four linear homogeneous equations for the unknown constants a_0, a_1, a_2, and a_3. Solutions exist only when the determinant of the matrix formed by the coefficients of these constants vanishes.

Since this determinant is implicitly a function of k and therefore λ, solutions λ_i^ν $(i=0,1,2,...,)$, for which the determinant vanishes, may be found numerically. The corresponding frequencies f_i^ν are then given by Eq. (33)

$$f_i^\nu=\frac{1}{2\pi}\sqrt{\frac{\lambda_i^\nu D}{m}}. \quad (36)$$

The fundamental frequency for each mode is determined by the smallest eigenvalue λ_0^ν.

Figure 4 shows dimensionless fundamental frequencies $\hat{f}_0^\nu\equiv f_0^\nu(mR^4/D)^{1/2}=(\lambda_0^\nu R^4)^{1/2}/2\pi$, as a function of μ, for the four lowest modes ($\nu=0,...,3$). For $\mu<0.39$, the lowest frequency mode is $\nu=1$ which corresponds to dipole distortions of the mirror. For the UBC/Laval 2.7-m telescope $\mu=0.15$ and the lowest frequency is $f_0^1=0.656(D/mR^4)^{1/2}$ which corresponds to 32 Hz for a 2 mm mercury load.

3. Stability

Instability can arise with a liquid mirror, because a local downward deflection of the surface results in a flow of liquid to that location, causing an increased pressure and further deflection (Content 1992). Consider a small deviation ζ of the surface from the equilibrium position which leaves the mean height of the surface unchanged (i.e., $\nu>0$). The change in pressure due to the mercury will be equal to $g\rho_{Hg}\zeta$, so from (11) we have

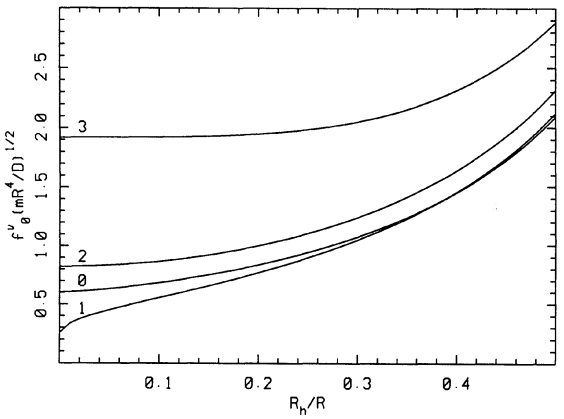

FIG. 4—Dimensionless resonant frequency $\hat{f}_0^\nu$, for the lowest four azimuthal modes, as a function of the relative hub diameter. Numbers labeling the curves refer to the mode number ν.

$$\Delta^2\zeta=\frac{g\rho_{Hg}}{D}\zeta, \quad (37)$$

which is an eigenvalue equation similar to (31). There will be a nontrivial solution ($\zeta\neq0$) only if $g\rho_{Hg}/D$ is an eigenvalue. The condition for stability, then, is

$$g\rho_{Hg}/D<\lambda_0, \quad (38)$$

where λ_0 is the smallest eigenvalue with $\nu>0$. In terms of the dimensionless *flexure coefficient* γ^ν, the stability criterion becomes

$$\gamma^\nu\equiv\frac{g\rho_{Hg}}{\lambda_0^\nu D}\leqslant1, \quad \text{for all } \nu>0. \quad (39)$$

In terms of the resonant frequency $\hat{f}_i^\nu$, we have

$$\gamma^\nu=\frac{g\rho_{Hg}R^4}{(2\pi\hat{f}_0^\nu)^2D}, \quad (40)$$

so flexure coefficients may be estimated for any μ from the curves in Fig. 4.

Consider now the effect of flexure of the mirror support system. An unbalanced load will result in a torque τ which will cause a flexure in the support system (including the bearing) resulting in a small tilt α in the vertical axis of the mirror. Because of this tilt, which we can take to be in the $\phi=0$ direction, there will be a redistribution of the mercury, resulting in a pressure $g\rho_{Hg}\alpha r\cos\phi$. The equilibrium equation (11) now gives

$$D\Delta^2\zeta=g\rho_{Hg}(\zeta+\alpha r\cos\phi). \quad (41)$$

The tilt angle α, however, is proportional to the torque

$$\tau=\int_0^{2\pi}\int_0^\infty Pr\cos\phi r\,dr\,d\phi$$
$$=D\int_0^{2\pi}\int_0^\infty\Delta^2\zeta r^2\,dr\cos\phi\,d\phi. \quad (42)$$

Let the constant of proportionality be κ^{-1} (κ is the moment stiffness of the support system), i.e., $\tau=\kappa\alpha$. Then (41) becomes

$$\Delta^2\zeta=\frac{g\rho_{Hg}}{D}\zeta+\frac{grho_{Hg}}{\kappa}r\cos\phi\int_0^{2\pi}\int_0^\infty\Delta^2\zeta r^2\,dr\cos\phi\,d\phi. \quad (43)$$

From the orthogonality of the trigonometric functions, the only contribution of the last term will be to the $\nu=1$ mode, so we substitute $\zeta=\chi^1\cos\phi$ in order to consider the effect of the support system flexure. Using $\Delta^2\chi^1\cos\phi=\lambda^1\chi^1\cos\phi$ we obtain

$$\lambda^1\chi^1=\frac{g\rho_{Hg}}{D}\chi^1+\frac{\pi g\rho_{Hg}}{\kappa}r\lambda^1M, \quad (44)$$

© Astronomical Society of the Pacific • Provided by the NASA Astrophysics Data System

1993PASP..105..501H

where

$$M=\int_0^\infty \chi^1 r^2\,dr. \tag{45}$$

Multiplying both sides of (44) by r^2 and integrating over r gives

$$\left[1-\frac{\pi g\rho_{\rm Hg}R^4}{4\kappa}-\frac{g\rho_{\rm Hg}}{\lambda^1 D}\right]M=0. \tag{46}$$

There will be a nontrivial solution if and only if the coefficient of M vanishes, which gives the stability criterion

$$\gamma_s+\gamma^1\leqslant 1, \tag{47}$$

where

$$\gamma^1=\frac{g\rho_{\rm Hg}}{\lambda_0^1 D}=\frac{g\rho_{\rm Hg}}{(2\pi\hat{f}_0^1)^2 D}, \tag{48}$$

and we have defined the flexure coefficient for the support system by

$$\gamma_s=\frac{\pi g\rho_{\rm Hg}R^4}{4\kappa}. \tag{49}$$

In order for the mirror to be stable, the total flexure coefficient $\gamma_s+\gamma^1$ must be less than unity.

REFERENCES

Arrien, F. 1990, B. Mech, thesis, Laval University, Quebec

Borra, E. F. 1982, JRASC, 76, 245

Borra, E. F. 1992a, Cassiopeia, 75, 4

Borra, E. F. 1992b, private communication

Borra, E. F., Content, R., Girard, L., Szapiel, S., Tremblay, L.-M., and Boily, E. 1992, ApJ, 393, 829

Borra, E. F., Content, R., Drinkwater, M. J., and Szapiel, S. 1989, ApJ, 346, L41

Content, R. 1992, Ph.D. thesis, Laval University, Quebec

Gibson, B. K., and Hickson, P. 1991, in The Space Distribution of Quasars, ed. D. Crampton (San Francisco, ASP), p. 80

Gibson, B. K., and Hickson, P. 1992, MNRAS, 258, 543

Hass, G., and Hadley, L. 1963, American Physics Institute Handbook (New York, McGraw–Hill)

Hickson, P. 1993, in preparation

Hickson, P., Gibson, B. K., Borra, E. F., Content, R., Girard, L., and Drinkwater, M. J. 1990, UBC technical report

Hickson, P., Narod, B., and Yedlin, M. J. 1993, in preparation

Landau, L. D., and Lifshitz, E. M. 1959, Theory of Elasticity, 3rd ed. (Oxford, Pergamon)

Marshall, A. C. 1989, Composite Basics, 2nd ed. (Walnut Creek, CA, Marshall Consulting)

McGraw, J. T., Angel, J. R. P., and Sargent T. A. 1980, in Applications of Digital Image Processing to Astronomy, ed. D. A. Eliot (Bellingham, SPIE), p. 20

Potter, A. E. 1991, private communication

Schultz, L. G. 1957, J. Opt. Soc. Am., 47, 64

Wright, J. F., and Mackay, C. D. 1981, in Solid State Imagers for Astronomy, ed. J. C. Geary and D. W. Latham (Bellingham, SPIE), p. 160

Vasil'ev, V. P. 1985, AZh, 62, 598

© Astronomical Society of the Pacific • Provided by the NASA Astrophysics Data System